

Article

# Design of Spatial-Mode (De)Multiplexer for Few-Mode Fibers Based on a Cyclically Used Michelson-Like Interferometer

Xesús Prieto-Blanco , Carlos Montero-Orille , Vicente Moreno de Las Cuevas ,  
María C. Nistal , Dolores Mouriz  and Jesús Liñares 

Quantum Materials and Photonics Research Group, Department of Applied Physics, Faculty of Physics/Faculty of Optics and Optometry, Universidade de Santiago de Compostela, Campus Vida s/n, E-15782 Santiago de Compostela, Galicia, Spain; carlos.montero@usc.es (C.M.-O.); vicente.moreno@usc.es (V.M.d.L.C.); mconcepcion.nistal@usc.es (M.C.N.); mariadolores.mouriz@usc.es (D.M.); suso.linares.beiras@usc.es (J.L.)

\* Correspondence: xesus.prieto.blanco@usc.es

Received: 25 October 2020; Accepted: 26 November 2020; Published: 30 November 2020



**Featured Application:** Spatial mode MUX/DEMUX for elliptical-core few-mode fibers in intra-datacenter networks.

**Abstract:** Few mode optical fibers are a promising way to continue increasing the data rate in optical communications. However, an efficient method to launch and extract separately each mode is essential. The design of a interferometric spatial mode (de)multiplexer for few mode optical fibers is presented. It is based on a single Michelson-like interferometer which consists of standard optical elements and has a reflective image inverter in one arm. Particular care has been taken in its design so that both polarizations behave the same. Moreover, this interferometer can process several pairs of modes simultaneously. The multiplexer also consists of: a phase plate, focusing optics at both ports of the interferometer and elliptical core fibers to recirculate some outputs. It can multiplex ten spatial and polarization modes and it presents low losses and no intrinsic crosstalk between modes. Additionally, it is polarization insensitive, achromatic, compact and inexpensive. The same system can work as a demultiplexer when used in reverse. In this case, both the losses and the crosstalk remain very low. Similar designs that perform other functions, like an add-drop mode multiplexing, are also suggested.

**Keywords:** optical fibers; space division multiplexing; few mode fibers; mode sorting; interferometers

## 1. Introduction

The use of optical fibers with a core having a few spatial propagation modes is a promising possibility of spatial division-multiplexing (SDM) to increase the transmission information rate of optical communications in order to meet future traffic demands [1,2]. Ideally, SDM must be orthogonal to polarization multiplexing and wavelength division multiplexing currently used, that is, each spatial mode must contain both polarizations and many wavelength channels spanning a few tens of nanometers in the spectrum. However, the crosstalk due to random mode mixing during the propagation along the fiber is an issue. It can be compensated by coherent detection and extensive use of multi-input-multiple-output (MIMO) digital signal processing (DSP) [3], although this solution requires carefully designed FMFs to obtain a low modal differential group delay. A more recent approach that is valid for short propagation distances is the use of elliptical core (EC) few mode fibers (FMF). These fibers not only significantly reduce crosstalk between both polarizations of the same mode (polarization maintaining) but also within the same spatial mode

group, such as  $LP_{11a}$  and  $LP_{11b}$ , since they are no longer degenerate. Therefore, MIMO and DSP can be removed from the detection stage. This solution has been proposed to improve the cabling footprint, bandwidth and link length of internal communications in data centers, while avoiding expensive and power-consuming detectors [4–6]. As MIMO is not present in these systems, a low mode crosstalk is also mandatory in mode (de)multiplexers. Multiplexing can be carried out in multiple ways, for instance by beam-splitters [7], Bragg gratings [8], directional couplers [9], photonic lanterns [10], multiplane light converters [11], or Mach-Zehnder interferometers (MZI) including Dove prisms to rotate the modes [12], a mirror image inverter [13], a refractive inverter [14] or a refractive Gouy’s phase retarder [15]. However, most of these methods have drawbacks for this application as shown in Table 1. Beam-splitters introduce high losses, the launched power being inversely proportional to the number of modes. Bragg gratings are wavelength sensitive. Directional couplers need 3D structures which are difficult to fabricate, or include mode rotators that are wavelength sensitive. Photonic lanterns currently have a notable crosstalk (around  $-6.5$  dB) Multiplane light conversion uses a complex phase plate which is difficult to design and fabricate; when implemented with a spatial light modulator, each polarization must be processed apart. Moreover, very large spectral ranges seem challenging to achieve with a diffractive method. Finally, multiplexers based on MZI are vibration-sensitive, difficult to align and bulky since they often need almost as many interferometers as modes to be multiplexed; besides, those based on reflections are polarization sensitive.

**Table 1.** Easily achievable characteristics of several spatial multiplexing methods.

	Beam Splitters	Bragg Gratings	Directional Couplers	Photonic Lanterns	Multiplane Converters	MZI with Dove Prisms	MZI with Mirror Inverter	MZI with Refractive Inverter	MZI with Gouy Phase	This Work
Theoretically lossless		✓	✓	✓	✓	✓	✓	✓	✓	✓
Polarization-insensitive	✓	✓	✓	✓				✓	✓	✓
Wavelength-insensitive	✓			✓		✓	✓	✓		✓
Low crosstalk	✓	✓	✓		✓	✓	✓	✓	✓	✓
Vibration-resistant	✓	✓	✓	✓	✓					✓
Simultaneous MUX of few modes				✓	✓		✓	†	†	✓
MUX of radial modes	✓		✓	✓	✓				✓	✓
Easy and cheap fabrication	✓					✓	✓	✓	✓	✓

† Only with cylindrical lenses.

In this work, we propose a new interferometric spatial mode (de)multiplexer for FMF. Besides the optical criteria (low light losses, achromatism, low crosstalk...), we also pay attention to other ones, such as number of elements, robustness, compactness and cost, in order to obtain a more attractive design for a practical use. On the contrary, we do not deal the issue of coupling efficiency of the modes to the fibres [16,17]. In Section 2, we present a modified Michelson interferometer with a mirror image inverter to demultiplex two spatial modes. In comparison with its MZI counterpart [13], it comprises less elements, it is monolithic and easier to align and especially it can manage both polarizations simultaneously in a no possible way with MZI. The modes coming from a fiber must be collimated before entering in the interferometer. The collimating system is dealt in Section 3 where we show that its focal length is fixed by the size of the interferometer. Next, in Section 4, the interferometer is used as a multiplexer adding a binary phase plate in one of its ports. Moreover, it can multiplex several pair of modes simultaneously. Better yet, we can multiplex four or five (for a more complex configuration) spatial modes in a few mode fiber with only one interferometer used in a cyclical

way. In addition, more complex operations are suggested to show the potential of this interferometer. Finally, the conclusions are presented in Section 5.

## 2. A Modified Michelson Interferometer as a Parity Selector

Let us consider that one of the mirrors of a Michelson interferometer is replaced with two perpendicular plane mirrors which form a hollow roof prism mirror whose edge is along the  $Y$ -axis as shown Figure 1. We also consider a zero path difference, which is achieved if the image of the prism edge through the beam splitter matches the plane mirror of the opposite arm. When an incoming plane wave illuminates this mirror normally, a uniform interference field is obtained at the output. In particular, by assuming an ideal phase change at each mirror reflection of  $\pi$  for TE polarization (electric field parallel to  $Y$ -axis), this configuration results in a destructive interference of the plane wave at the output port opposite to the light source because one reflection more occurs in the arm containing the hollow roof prism. Now, let us consider an incident wave whose amplitude changes slowly along its wavefront. The hollow roof mirror spatially inverts the wavefront, exchanging its right and left sides symmetrically around its edge. That is of no consequence if the wave has also a symmetrical amplitude, for example a gaussian beam centred on the edge. However, if the wave amplitude is antisymmetric (such as in an odd Hermite-Gaussian beam), the spatial inversion is equivalent to a sign change of the amplitude, that is, to an extra  $\pi$  phase. Therefore the antisymmetric waves will interfere destructively in the source port and constructively in the opposite one, unlike the symmetrical waves do. In order to avoid that the symmetric wavefronts return exactly to the light source, the incoming wave must propagate slightly out of the  $XZ$ -plane. In other words, the rays shown in Figure 1 actually are the projections of real rays on the  $XZ$ -plane.

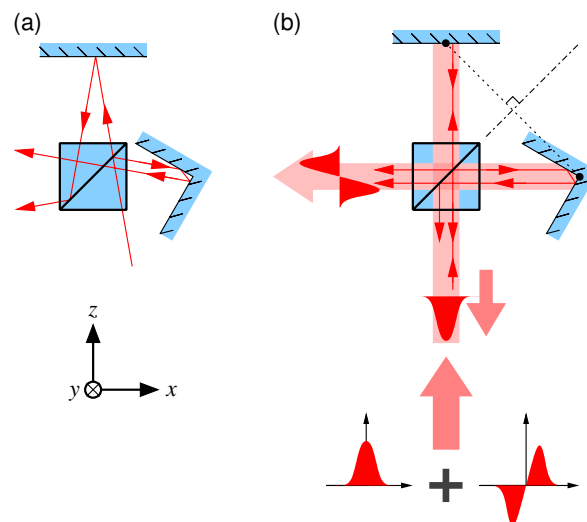


**Figure 1.** (a) Michelson interferometer with a hollow roof mirror. (b) The zero path difference is indicated by the dotted line. The behavior for TE polarization assuming reflection phases of  $\pi$  is shown for different transverse fields.

In short, this Michelson interferometer separates the symmetric and antisymmetric part of the incoming TE-polarized wave, sending each part to a different exit port. Conversely, the same interferometer acts as multiplexer when symmetric and antisymmetric wavefronts enter from different ports.

For TM polarization, the reflection phases at metal mirrors are near zero; consequently symmetrical and antisymmetric wavefronts emerge from exchanged ports with respect to the TE case. In order to make a polarization-insensitive (de)multiplexer, a quarter-wave plate have to be included in one arm of the interferometer. As the wave crosses twice this plate, it introduces another  $\pi$

phase between both polarizations. Thus, they will become synchronized, that is, both polarizations will interfere constructively in the same output port for the same wavefront.

### Non-Ideal Mirrors

When we take into account the non-ideal reflectance of the metal mirrors, the amplitudes of the interfering waves become unbalanced and the phase difference is not exactly 0 or  $\pi$  for the zero geometrical path difference configuration. Consequently, the destructive interferences are not complete, which results in a crosstalk between symmetrical and antisymmetric wavefronts. The phase difference can usually be compensated with geometrical path for a monochromatic source. However, in our case, it can not be done simultaneously for both polarizations since the difference between their reflection phases at an incidence of  $45^\circ$  is not exactly  $\pi$ , unlike in normal incidence (Table 2). Instead it is  $185.27^\circ$  for aluminium and  $188.02^\circ$  for silver; these mismatches have a greater influence in crosstalk than the amplitude difference of waves from both arms. Indeed, the interfering TE waves emerging from the opposite port to the source are proportional to:

$$t_{\perp}^{BS} r_{\perp 0} r_{\perp}^{BS} \quad \text{and} \quad r_{\perp}^{BS} r_{\perp 45}^2 t_{\perp}^{BS} e^{i2kd},$$

where  $t_{\perp}^{BS}$  and  $r_{\perp}^{BS}$  are the Fresnel's transmittance and reflectance coefficients of the beam-splitter;  $r_{\perp 0}$  ( $r_{\perp 45}$ ) is the Fresnel coefficient of the mirrors at normal ( $45^\circ$ ) incidence;  $k$  is the wavenumber; and  $d$  is the arm length difference. The amplitude of the interference is proportional to the sum of those values for symmetric wavefronts; but it is their difference if the wavefront is antisymmetric. Therefore the ratio of intensities between symmetric and antisymmetric wavefronts (crosstalk) is:

$$\left| \frac{r_{\perp 0} + r_{\perp 45}^2 e^{i2kd}}{r_{\perp 0} - r_{\perp 45}^2 e^{i2kd}} \right|^2 \simeq \left| \frac{1 + e^{i(2\phi_{\perp 45} - \phi_{\perp 0} + 2kd)}}{1 - e^{i(2\phi_{\perp 45} - \phi_{\perp 0} + 2kd)}} \right|^2,$$

where we have neglected the mirror absorptions:

$$\begin{aligned} r_{\perp 0} &= |r_{\perp 0}| e^{i\phi_{\perp 0}} \simeq e^{i\phi_{\perp 0}}, \\ r_{\perp 45} &= |r_{\perp 45}| e^{i\phi_{\perp 45}} \simeq e^{i\phi_{\perp 45}}. \end{aligned}$$

This ratio cancels if argument of the complex exponentials is a odd multiple of  $\pi$ :

$$2\phi_{\perp 45} - \phi_{\perp 0} + 2kd = (2m + 1)\pi \quad m \in \mathbb{Z}.$$

Since  $\phi_{\perp 45} \simeq \phi_{\perp 0} \simeq -\pi$ , the solution for the smallest  $d$  happens for  $m = -1$ :

$$2\phi_{\perp 45} - \phi_{\perp 0} + 2kd = -\pi. \tag{1}$$

Analogously, the crosstalk for TM polarization is given approximately by:

$$\left| \frac{1 + e^{i(2\phi_{\parallel 45} - \phi_{\parallel 0} + 2kd + \pi)}}{1 - e^{i(2\phi_{\parallel 45} - \phi_{\parallel 0} + 2kd + \pi)}} \right|^2$$

where a  $\pi$  phase was included to account for the twice crossed  $\lambda/2$  wave plate. In this case, the smaller  $d$  that cancels the last ratio is:

$$2\phi_{\parallel 45} - \phi_{\perp 0} + 2kd = \pi, \tag{2}$$

where the relationship:  $\phi_{\parallel 0} - \phi_{\perp 0} = \pi$  was used. As Equations (1) and (2) are not compatible, we can choose the mean value for  $d$  as a trade-off:

$$2kd = \phi_{\perp 0} - \phi_{\perp 45} - \phi_{\parallel 45}.$$

Therefore, we obtain the same crosstalk for TE and TM polarizations:

$$\left| \frac{1 + e^{\pm i(\phi_{\parallel 45} - \phi_{\perp 45})}}{1 - e^{\pm i(\phi_{\parallel 45} - \phi_{\perp 45})}} \right|^2 = \frac{1}{\tan^2 \frac{\phi_{\parallel 45} - \phi_{\perp 45}}{2}}.$$

By replacing  $\phi_{\parallel 45}$  and  $\phi_{\perp 45}$  with the values of Table 2, the crosstalk between symmetric and antisymmetric wavefronts achieves  $-26.7$  dB and  $-23.0$  dB for aluminium and silver mirrors respectively. These values are rather modest as theoretical limits. To improve them, a custom retarder wave plate should be made to finely synchronize TE and TM polarizations; but this solution is cumbersome.

**Table 2.** Amplitude and phase changes acquired after a reflection in some dielectric-metal interfaces at  $\lambda = 1550$  nm. The following complex refractive indices [18] were assumed:  $n_{Ag} = 0.40960 + 10.048i$ ,  $n_{Al} = 1.5137 + 15.234i$ ,  $n_{BK7} = 1.5007 + 1.4361 \cdot 10^{-7}i$ .

Incidence		Polarization			
		$r_{\perp}$ (TE)		$r_{\parallel}$ (TM)	
		$ r_{\perp} $	$\phi_{\perp}$ (°)	$ r_{\parallel} $	$\phi_{\parallel}$ (°)
Air-Al	normal	0.9872	$-172.56$	0.9872	7.44
	at 45°	0.9910	$-174.74$	0.9820	10.52
Air-Ag	normal	0.9920	$-168.65$	0.9920	11.35
	at 45°	0.9944	$-171.98$	0.9887	16.04
BK7-Ag	normal	0.9882	$-163.04$	0.9882	16.96
	at 45°	0.9917	$-168.03$	0.9834	23.94
BK7-Al	normal	0.9810	$-168.86$	0.9810	11.14
	at 45°	0.9865	$-172.13$	0.9733	15.75

Instead, we propose the inclusion of a mirror oriented at 45° in the arm that only had one mirror as shown in Figure 2a. This compensates for the phases and the amplitude losses of the hollow roof prism at any wavelength. The mirror illuminated under normal incidence remains uncompensated, but its reflection phases for TE and TM polarization differs exactly 180°, therefore a standard quarter wave retarder is enough to adjust them. In particular, we propose a Fresnel retarder because it is achromatic, and it is advisable that this device works in a band as wide as possible. Moreover, its dispersion can also be compensated in the other arm with a piece of the same glass type with the proper length. To be more specific, the exact crosstalk for TE polarization is now:

$$\left| \frac{r_{\perp 0} + e^{i2kd}}{r_{\perp 0} - e^{i2kd}} \right|^2 = \left| \frac{|r_{\perp 0}| + e^{i(2kd - \phi_{\perp 0})}}{|r_{\perp 0}| - e^{i(2kd - \phi_{\perp 0})}} \right|^2.$$

Analogously, the crosstalk for TM polarization is:

$$\left| \frac{r_{\parallel 0} + e^{i(2kd + \pi)}}{r_{\parallel 0} - e^{i(2kd + \pi)}} \right|^2 = \left| \frac{|r_{\parallel 0}| + e^{i(2kd + \pi - \phi_{\parallel 0})}}{|r_{\parallel 0}| - e^{i(2kd + \pi - \phi_{\parallel 0})}} \right|^2,$$

but taking into account that  $|r_{\parallel 0}| = |r_{\perp 0}|$  and  $\phi_{\parallel 0} - \phi_{\perp 0} = \pi$ , it results that both conditions are the same. They are minimized simultaneously when:

$$2kd = \phi_{\parallel 0},$$

and the residual crosstalk is governed by  $|r_{\parallel 0}|$ , being:

$$\left| \frac{|r_{\parallel 0}| - 1}{|r_{\parallel 0}| + 1} \right|^2, \tag{3}$$

which leads to much better results:  $-47.9$  dB for a silvered mirror and  $-43.8$  dB for an aluminized one. Importantly, the key to easily synchronizing both polarizations is that the uncompensated reflection occurs at normal incidence, which is not possible in an MZI. The crosstalk in the exit port that is opposite to the source (Equation (3)) is independent of the beam-splitter specifications because the wave from each arm is transmitted and reflected once at it. However, the light returning to the source port is the result of the interference of a wave reflected twice with another transmitted twice by the beam-splitter. So, if  $t^{BS} \neq r^{BS}$ , their amplitudes are unbalanced which prevents the full destructive interference and increases the crosstalk. Fortunately, a difference of 1% between reflectance and transmittance (which can be achieved with commercial beam-splitters) leads to a crosstalk better than  $-39$  dB, a value almost as good as that of the other port.

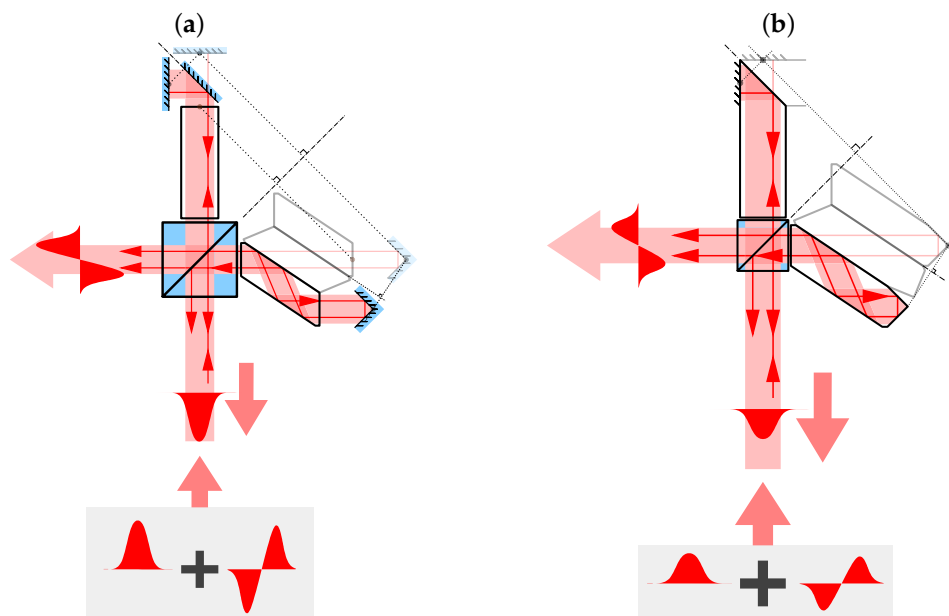


**Figure 2.** (a) Proposed interferometer which comprises a Fresnel retarder to synchronize both polarizations in the arm containing the hollow roof prism and both a glass plate and a  $45^\circ$  metallic mirror in the other arm as compensating elements. The unfolded paths are shown in light colours. (b) A more compact interferometer by using total internal reflection.

A variant of this interferometer is shown in Figure 2b, where the hollow roof mirror was replaced with a Porro's prism (let us assume that it is made of BK7 glass) which works under total internal reflection. Note that the phases introduced by these total reflections at  $45^\circ$  are far away from zero or  $\pi$ , but again they are exactly compensated by those appearing in the total internal reflections of the other arm. In this case, the crosstalk is also given by Equation (3), but being  $r_{\parallel 0}$  the Fresnel coefficient for the interface glass-metal. Although the crosstalk is slightly worse than the previous one, it is still theoretically high:  $-44.5$  dB for silver and  $-40.3$  dB for aluminium. Moreover, the Fresnel prism and the compensator can be glued to the beam splitter with optical cement to form a compact,

vibration-insensitive monolithic system. All of these modifications also eliminate or reduce reflection losses in mirrors, the beam splitter, the Fresnel prism and the compensator without using expensive anti-reflective coatings. Of course, the theoretical performance of the system can be improved further, at the expense of cost, with a mirror and beam splitter having all-dielectric reflecting surfaces. However, it is difficult to achieve such good values in real systems. In a previous work [14], we have achieved experimental crosstalk of around  $-14$  dB, but it can be improved as we do not balance the losses of both arms. On the other hand, Igarashi et al. [13] have obtained crosstalk as low as  $-24$  dB with an MZI. We expect that similar values can be achieved with our Michelson interferometer.

### 3. Collimating System

In order to separate symmetric and antisymmetric (along  $X$ -axis) modes of a multimode fiber, we need to collimate the beam from the fiber with a positive lens and then to introduce it in one of the above interferometers. In the simplest case, the fiber optical axis is aligned parallel to the  $Z$ -axis and its  $X$ -coordinate is determined by the interferometer since the projection of the rays on the  $XZ$ -plane must fall normally on the plane mirror. However, the  $Y$ -coordinate of the fiber axis is essentially free. It is only limited by phase changes in the Fresnel retarder and in the plane mirror reflections, but both of them depend quadratically on the  $Y$ -coordinate of the fiber, so we will ignore in our analysis.

We are interested in coupling the output waves from both ports into new fibers. The beam returning to the source port is focused by the collimating lens symmetrically along the  $Y$ -axis, where the end face of an output fiber must be located (Figure 3a). However, the principal ray of the beam should propagate parallel to the optical axis of this fiber in order the light remains coupled to the same mode than it did in the input fiber. For example, let suppose that the interferometer send the fundamental mode of the input fiber ( $LP_{01}$ ) to the source port. If this beam illuminates the output fiber with a tilt, it will partially couple to the second mode antisymmetric along  $Y$  ( $LP_{11b}$ ) because a tilted illumination is equivalent to a linear phase along the  $Y$ -axis. It does not introduce crosstalk with the light from the other port which couples to the antisymmetric modes along  $X$  (for example  $LP_{11a}$ ). But it does introduce crosstalk between modes when two interferometers (as those presented in the next section) are concatenated. The easiest way to avoid that, is to put both fibers parallel and to accomplish that the principal ray also returns from the interferometer parallel to its input direction. The last condition is achieved when the focal plane of the system composed by the collimating lens, the beam-splitter and the compensating plate matches the plane mirror (Figure 3b). Consequently, the focal plane also contains the vertex of the hollow roof prism (or the Porro's prism) in the other arm.

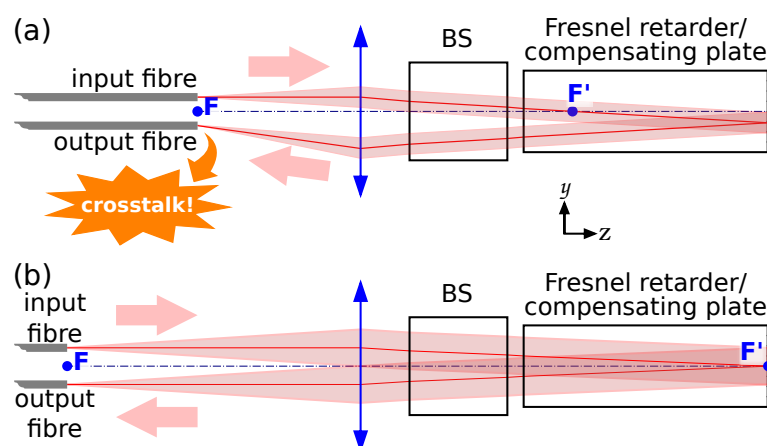


**Figure 3.** Lateral view of an arm of the interferometer and a lens to collimate the light emerging from a fiber. The same collimating lens does not couple correctly the light into an output fiber (a), unless the principal ray of the returning beam was aligned with the fiber axis (b).

An identical lens must be symmetrically located respect to the beam-splitter to couple the wave emerging from the other output port of the interferometer in other fiber. A perspective view of this system is shown in the bottom interferometer of Figure 4. As there is a degree of freedom in the Y-coordinate of the fibers, several signals can be (de)multiplexed simultaneously. In this figure, a phase plate was also included in port P1 between the lens and the beam-splitter. Its function is explained in the following section.

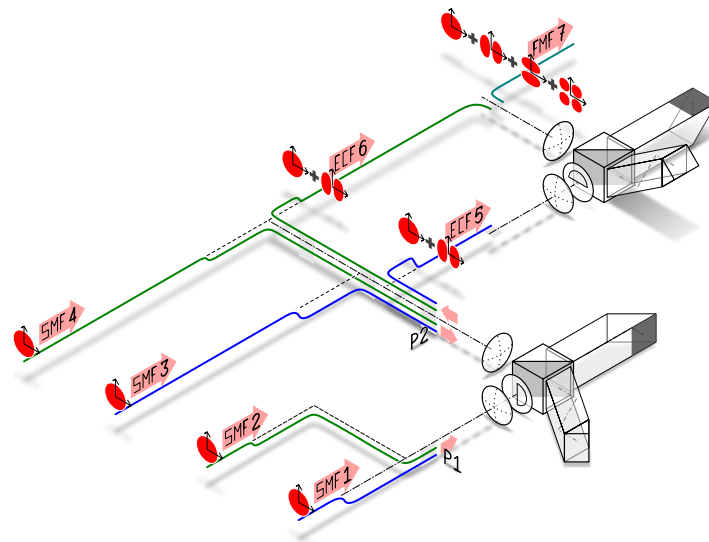


**Figure 4.** Two concatenated interferometers to multiplex four modes into a few mode fiber.

#### 4. Multiplexers Based on Cyclically Used Michelson Interferometers

A multiplexer based on two interferometers similar to the one of the previous section is shown in Figure 4. It multiplexes the signal from four single mode fibers into respective spatial modes of a few mode fiber. The bottom interferometer includes a phase plate in one of its ports (P1), which introduces a  $\pi$ -phase in the right side of the wavefronts coming from fiber 1, leading to an antisymmetric amplitude along X-axis. The length of the arms must be adjusted to obtain fully constructive interference in the other port (P2). The light from the single mode fiber 3 (symmetric amplitude from P2) also exits through P2, leading to a first multiplexing. These signals are coupled into fiber 5, which must support two modes along the horizontal direction. The amplitude unbalance due to the uncompensated reflection hardly matters when the interferometers are used as multiplexers. This unbalance generates a low intensity wave in the exit of port P1 which is unused. Therefore there is a little efficiency reduction in the multiplexed output, but no crosstalk appears. Similarly, a misalignment of the phase plate or a deviation of its phase shift from  $\pi$  due to chromatic dispersion [19] introduces a small symmetrical wave component into the interferometer, but it is sent back to port P1, that is, it does not generate crosstalk on port P2 either. Analogously, the signals from fibers 2 and 4 are combined and coupled to respective modes of the fiber 6. Both fibers 5 and 6 must maintain an horizontal orientation of the second mode. In theory, it can be done with circular core fibers provided that the curves they describe avoid topological coupling between modes. However, EC-FMFs accomplish this task more easily if the long axes of its cores are oriented horizontally (or vertically) at both ends [4]. Remember that these fibers also maintain the beam polarization.

The second interferometer (top-right in Figure 4) is similar to the first one, but it multiplexes symmetric and antisymmetric amplitudes along the vertical direction. To do that, the phase plate, the Porro's prism and the compensating prism are rotated 90 degrees; moreover the fiber ends are displaced horizontally (instead of vertically) with respect to the optical axes of the collimating lenses. The beams from fiber 5 are coupled in the antisymmetric modes along Y-axis of the final few mode

fiber 7. Although this multiplexer does not cyclically use any interferometer, it is a good introduction to the following system.

We can save the last interferometer if the output of fibers 5 and 6 are rotated 90 degrees and then they are introduced again into the first interferometer. In Figure 5 one can see this cyclically used interferometer. Similarly to the MZI with reflective image inverters [13], this interferometer also can multiplex 5 spatial modes instead of 4, albeit in somewhat more complicated scheme as shown in Figure 6. Note that the mode from the fiber SMF3 of Figure 5 never crosses the phase plate, so it generates the fundamental mode of FMF7 output. If we could add a  $LP_{21a}$  mode (symmetrical along X and Y directions) in SMF3, it would behave like the fundamental mode in each multiplexing operation, exiting the interferometer together the other four modes. To that end, we can multiplex  $LP_{01}$  and  $LP_{21b}$  modes into an elliptical core fiber by using the interferometer, rotate them  $45^\circ$  to generate the  $LP_{21a}$  mode, and replace the SMF3 with this fiber. The  $LP_{21b}$  mode can be generated from a  $LP_{11b}$  one (antisymmetric along vertical direction) entering by port P1 while the  $LP_{01}$  mode enters by port P2. Finally, the  $LP_{11b}$  mode is previously obtained from a  $90^\circ$ -rotated  $LP_{11a}$  one emerging from the interferometer when a  $LP_{01}$  mode from a new single mode fiber is introduced into P1. In short, the final  $LP_{21a}$  mode is obtained after four passes through the interferometer: two of them to obtain the mode itself and multiplex it with the final  $LP_{01}$  mode and the last two passes to multiplex them with the other three modes.

It is worth highlight that we can remove the phase plates from these systems and to replace the input single mode fibers with few mode fibers. In this case there is no mode conversion but each mode can be managed separately. So we can do the (de)multiplexing and the mode conversion (if necessary) in two different stages. For example we can drop and add a mode of a few mode fiber with two systems similar to that of Figure 5 without phase plate. The first one should act as a demultiplexer putting each mode in its respective fiber from 1 to 4 (now few mode fibers). The desired mode is extracted (drop) and the rest are coupled to the corresponding inputs of the second system which acts as a multiplexer. We can introduce a new signal (add) in the proper mode of the free input fiber of the second system. The new signal will be incorporated with the other three in the output few mode fiber. Even more, both systems can be merged into one by sharing the interferometer, doubling the number of fibers in each port and connecting them properly.

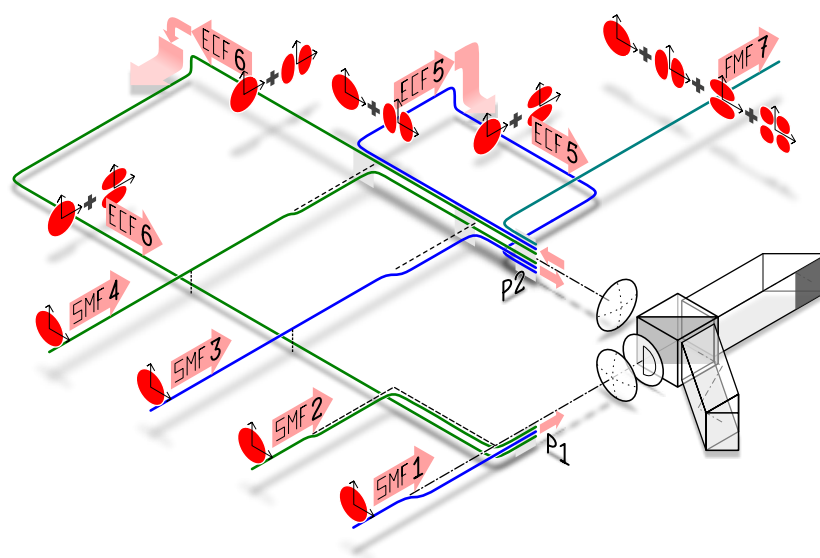
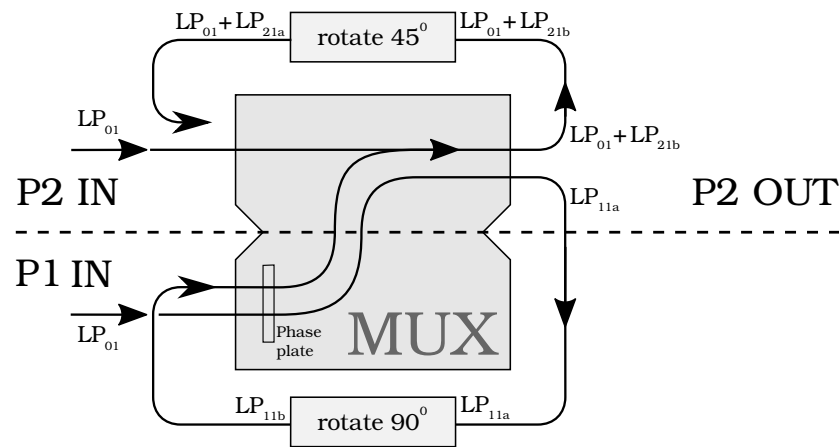


Figure 5. Multiplexer similar to that of Figure 4, but cyclically using a single interferometer.



**Figure 6.** Generation of a  $LP_{21a}$  mode multiplexed with a  $LP_{01}$  mode. The gray box represents the multiplexer of Figure 5. The lines are new recirculating fibers when are out of the box and free space modes inside it. The lower half of the box is port P1 and the upper half is P2, with the input on the left and the output on the right. If we replace the fiber SM3 of Figure 5 with the one containing the multiplexed modes  $LP_{21a}$  and  $LP_{01}$ , we will obtain five spatial modes in FMF7.

Other interferometric multiplexers based on MZI can be redesigned as Michelson interferometers. However, the interferometers using two Dove prisms [12] or those based on image inversion with spherical lenses can not multiplex several pair of modes simultaneously, because the emerging beams are parallel only if the input fiber is on the optical axis. Therefore they can not be used cyclically. On the contrary, those using cylindrical lenses, for instance in order to generate an image inversion in only one direction, do can multiplex several pairs of modes since they have an invariant behavior along the perpendicular direction. Similarly the refractive Gouy phase shifters with cylindrical lenses [15] can take advantage of this cyclic use to enlarge the SDM to radial modes more economically. Their adaptation to the Michelson configuration requires two simple modifications. First, the collimating system must now generate a slightly convergent beam whose waist must be located at the reference mirror. And secondly, just the cylindrical lens must be inserted at the proper distance of the mirror of the other arm. Note that since only one reflection occurs in each arm, the interferometer is already polarization insensitive, so the Fresnel retarder is unnecessary in this case.

## 5. Conclusions

Although there are several proposals for spatial mode (de)multiplexers for few mode fiber communications, new achromatic and polarization-independent designs are necessary to spatial division multiplexing achieves commercial use in combination with polarization and wavelength division multiplexing. Our demultiplexer, unlike other interferometric ones, is based on a Michelson-like interferometer. It uses a reflective image inverter made by a hollow roof prism mirror or a roof prism in an arm instead of the usual mirror, in such a way that symmetric and antisymmetric modes exit by opposite ports. In order for the system to behave the same for the two polarizations some elements are included. A  $\lambda/4$  retarder must be introduced in an arm, in particular, a Fresnel retarder is desirable as it is achromatic. Besides, any other non-normal incidence in an arm is compensated in the other one with an identical incidence. Such a compensation is not possible in a Mach-Zehnder configuration. A lens in each port is needed to collimating the light from the respective input fibers and focusing it in the output fiber. To minimize the crosstalk between modes, the focal planes of these lenses must match both the mirror and the vertex of the roof prism. The residual crosstalk depends on the quality of the mirrors and the beam splitter.

If a phase plate is included in the proper port, the system works as a multiplexer that transform the modes of two single mode fibers into two modes (one symmetric and the other antisymmetric) of a few mode fiber. The plate can introduce some losses, but not crosstalk. As the image inverter has

translation symmetry perpendicularly to the inversion direction, the signal of several pairs of fibers can be multiplexed to the respective output fibers simultaneously with the same interferometer. Besides, these output signals are coupled to few mode elliptical core fibers and recirculated to other inputs. Taking advantage of the fact that the orientation of the modes of these fibers is easily controllable, five spatial modes can be multiplexed in a few mode fiber with a single interferometer. An add-drop mode multiplexer and other configurations based in the same interferometer are suggested.

In short, we have designed a five spatial mode (de)multiplexer which is achromatic, polarization-insensitive and presents low losses and very low crosstalk. This design can be modified in several ways, so it could be a powerful tool for mode multiplexing.

**Author Contributions:** All authors have contributed equally to this work. All authors have read and agreed to the published version of the manuscript.

**Funding:** This research was funded by: Ministerio de Economía, Industria y Competitividad, Gobierno de España, grant number AYA2016-78773-C2-2-P; Xunta de Galicia, Consellería de Educación, Universidades e FP, Grant GRC number ED431C2018/11; and European Regional Development Fund.

**Conflicts of Interest:** The authors declare no conflict of interest. The funders had no role in the design of the study; in the collection, analyses, or interpretation of data; in the writing of the manuscript, or in the decision to publish the results.

## Abbreviations

The following abbreviations are used in this manuscript:

SDM	Spatial division multiplexing
MIMO	Multiple input multiple output
DSP	Digital signal processing
FMF	Few-mode fiber
SMF	Single mode fiber
EC	Elliptical core
MZI	Mach-Zehnder interferometer
TE	Transverse electric
TM	Transverse magnetic

## References

- Li, G.; Bai, N.; Zhao, N.; Xia, C. Space-division multiplexing: the next frontier in optical communication. *Adv. Opt. Photon.* **2014**, *6*, 413–487. [[CrossRef](#)]
- Ryf, R.; Fontaine, N.K. Space-Division Multiplexing and MIMO Processing. In *Enabling Technologies for High Spectral-Efficiency Coherent Optical Communication Networks*; Zhou, X., Xie, C., Eds., Wiley Telecom: Hoboken, NJ, USA, 2016; pp. 547–608.
- Ryf, R.; Randel, S.; Gnauck, A.H.; Bolle, C.; Sierra, A.; Mumtaz, S.; Esmaeelpour, M.; Burrows, E.C.; Essiambre, R.; Winzer, P.J.; et al. Mode-Division Multiplexing Over 96 km of Few-Mode Fiber Using Coherent  $6 \times 6$  MIMO Processing. *J. Lightwave Technol.* **2012**, *30*, 521–531. [[CrossRef](#)]
- Ip, E.; Milione, G.; Li, M.J.; Cvijetic, N.; Kanonakis, K.; Stone, J.; Peng, G.; Prieto, X.; Montero, C.; Moreno, V.; et al. SDM transmission of real-time 10GbE traffic using commercial SFP + transceivers over 0.5 km elliptical-core few-mode fiber. *Opt. Express* **2015**, *23*, 17120–17126. [[CrossRef](#)] [[PubMed](#)]
- Parmigiani, F.; Jung, Y.; Grüner-Nielsen, L.; Geisler, T.; Petropoulos, P.; Richardson, D.J. Elliptical Core Few Mode Fibers for Multiple-Input Multiple Output-Free Space Division Multiplexing Transmission. *IEEE Photonics Technol. Lett.* **2017**, *29*, 1764–1767. [[CrossRef](#)]
- Zhang, L.; Chen, J.; Agrell, E.; Lin, R.; Wosinska, L. Enabling Technologies for Optical Data Center Networks: Spatial Division Multiplexing. *J. Lightwave Technol.* **2020**, *38*, 18–30. [[CrossRef](#)]
- Bai, N.; Ip, E.; Huang, Y.K.; Mateo, E.; Yaman, F.; Li, M.J.; Bickham, S.; Ten, S.; Liñares, J.; Montero, C.; et al. Mode-division multiplexed transmission with inline few-mode fiber amplifier. *Opt. Express* **2012**, *20*, 2668–2680. [[CrossRef](#)] [[PubMed](#)]

8. Han, Y.; Hu, G. A novel MUX/DEMUX based on few-mode FBG for mode division multiplexing system. *Opt. Commun.* **2016**, *367*, 161–166. [[CrossRef](#)]
9. Hanzawa, N.; Saitoh, K.; Sakamoto, T.; Matsui, T.; Tsujikawa, K.; Koshihara, M.; Yamamoto, F. Mode multi/demultiplexing with parallel waveguide for mode division multiplexed transmission. *Opt. Express* **2014**, *22*, 29321–29330. [[CrossRef](#)] [[PubMed](#)]
10. Leon-Saval, S.G.; Fontaine, N.K.; Salazar-Gil, J.R.; Ercan, B.; Ryf, R.; Bland-Hawthorn, J. Mode-selective photonic lanterns for space-division multiplexing. *Opt. Express* **2014**, *22*, 1036–1044. [[CrossRef](#)] [[PubMed](#)]
11. Labroille, G.; Denolle, B.; Jian, P.; Genevaux, P.; Treps, N.; Morizur, J.F. Efficient and mode selective spatial mode multiplexer based on multi-plane light conversion. *Opt. Express* **2014**, *22*, 15599–15607. [[CrossRef](#)] [[PubMed](#)]
12. Boffi, P.; Martelli, P.; Gatto, A.; Martinelli, M. Mode-division multiplexing in fibre-optic communications based on orbital angular momentum. *J. Opt.* **2013**, *15*, 075403. [[CrossRef](#)]
13. Igarashi, K.; Souma, D.; Takeshima, K.; Tsuritani, T. Selective mode multiplexer based on phase plates and Mach-Zehnder interferometer with image inversion function. *Opt. Express* **2015**, *23*, 183–194. [[CrossRef](#)] [[PubMed](#)]
14. Liñares, J.; Prieto-Blanco, X.; Moreno, V.; Montero-Orille, C.; Mouriz, D.; Nistal, M.C.; Barral, D. Interferometric space-mode multiplexing based on binary phase plates and refractive phase shifters. *Opt. Express* **2017**, *25*, 10925–10938. [[CrossRef](#)] [[PubMed](#)]
15. Liñares, J.; Prieto-Blanco, X.; Montero-Orille, C.; Moreno, V. Spatial mode multiplexing/demultiplexing by Gouy phase interferometry. *Opt. Lett.* **2017**, *42*, 93–96. [[CrossRef](#)] [[PubMed](#)]
16. Igarashi, K.; Souma, D.; Tsuritani, T.; Morita, I. Performance evaluation of selective mode conversion based on phase plates for a 10-mode fiber. *Opt. Express* **2014**, *22*, 20881–20893. [[CrossRef](#)] [[PubMed](#)]
17. Liñares, J.; Montero-Orille, C.; Moreno, V.; Mouriz, D.; Nistal, M.C.; Prieto-Blanco, X. Ion-exchanged binary phase plates for mode multiplexing in graded-index optical fibers. *Appl. Opt.* **2017**, *56*, 7099–7106. [[CrossRef](#)] [[PubMed](#)]
18. Polyanskiy, M.N. Refractive Index Database. Available online: <http://refractiveindex.info> (accessed on 16 February 2015).
19. Prieto-Blanco, X.; Montero-Orille, C.; Moreno, V.; Mateo, E.F.; Liñares, J. Chromatic characterization of ion-exchanged glass binary phase plates for mode-division multiplexing. *Appl. Opt.* **2015**, *54*, 3308–3314. [[CrossRef](#)] [[PubMed](#)]

**Publisher's Note:** MDPI stays neutral with regard to jurisdictional claims in published maps and institutional affiliations.



© 2020 by the authors. Licensee MDPI, Basel, Switzerland. This article is an open access article distributed under the terms and conditions of the Creative Commons Attribution (CC BY) license (<http://creativecommons.org/licenses/by/4.0/>).